

CAN WE PREDICT THE SINTERING KINETICS OF PORCELAIN STONEWARE? THE CASE OF GLASSY WASTE-BASED BODIES

**Sonia Conte, Chiara Zanelli, Chiara Molinari, Guia Guarini,
Michele Dondi**

CNR-ISTEC, via Granarolo 64, 48018 Faenza, Italy

ABSTRACT

The production of ceramic tiles is continuously increasing worldwide, involving a growing demand for raw materials. On the other hand, the progressive depletion of the main feldspathic flux deposits is forcing the ceramic industry to search for suitable substitutes. Although the tile-making industry has proven able to recycle its own processing residues, the use of wastes from further sources is at present quite limited. The use of glassy wastes, for instance, is usually hindered for technological reasons: a

low-melting glass can significantly affect the firing behavior and particularly high temperature permanent deformations. The main goal of this study is therefore to assess the firing behavior of porcelain stoneware bodies containing glassy wastes, and particularly to verify if the sintering kinetics can be satisfactorily predicted applying the well-known models inherited from the glass densification theory, such as the Frenkel model. Five different sources (bottle, PC-TV screen, lamp, glaze manufacturing and porcelain stoneware grinding sludge) provided glassy wastes that were separately added to a reference body in an amount of 20%. Each batch was characterized from the chemical point of view and its sintering kinetics were determined in isothermal conditions by optical thermo-dilatometric analysis (TA ODP868). The isothermal tests were carried out at T_{gr} (gresification temperature) with a heating rate of 80°C/min up to T_{gr} and 30 min dwell time. The quantitative phase composition after firing at T_{gr} was determined by XRD-Rietveld in order to calculate the chemical and physical properties of the vitreous phase. Shear viscosity and liquid-air surface tension were used as input of the Frenkel model to calculate the initial sintering rate of the bodies. Such calculated sintering rates were then compared with the experimental rates derived from the sintering curves. The introduction of a certain amount of glass into a porcelain stoneware body determines a clear change in the sintering mechanism. The waste-free batch behaves substantially in agreement with the Frenkel model, confirming that the initial sintering rate is fundamentally governed by the physical properties of the liquid phase. However, the addition of 20% glass is reflected by a significant deviation from the behavior of the benchmark, which sees the Frenkel model failing to predict accurately the sintering rate on the basis of melt viscosity and surface tension just in two cases.

1. INTRODUCTION

The production of ceramic tiles is continuously increasing worldwide reaching over 13.5 billion square meters in 2017 [1]. This involves a growing demand for raw materials, attaining an estimated global consumption beyond 250 million tons per year. This picture represents a challenge for the ceramic industry with a view to making tile manufacturing fully sustainable in the long run, especially in the transition towards a Circular Economy [2].

The ceramic industry has proven able to recycle its own processing residues into cannibalistic loops to large extent. Best available technologies allow an index of reuse close to 100% to be achieved for in-house wastes from milling, pressing, drying and glazing and even over 100% in the case a tile-making line utilizes residues from other factories [3].

Although the recourse to residues from other industrial sectors or from municipal waste sorting has already entered industrial practice, the actual utilization is quite limited in ceramic production. Despite there being a large amount of literature data available on waste recycling [4], industrial use is nowadays essentially restricted to soda-lime glass and occasionally further glasses and sanitaryware scraps (few percent units in the batch). Some technological drawbacks are known, concerning especially the control of firing behavior and pyroplasticity [4-6], but they are apparently counterbalanced by advantages in terms of energy consumption, stemming from lower firing temperatures. However, the literature results differ regarding the amount of waste glass that can be tolerated in porcelain stoneware bodies, and its effects on technological behavior and technical performance of ceramic tiles. Besides a general convergence towards a "fluxing effect" of waste glasses, it is not clear what the influence

is on phase composition, as well as on the composition and physical properties of the vitreous phase, and eventually the sintering mechanisms and kinetics [4-8]. Therefore, it is crucial to better understand how waste glasses behave during firing.

Fortunately, the firing behavior of porcelain stoneware has been extensively investigated, leading to a phenomenological outline of its viscous flow sintering, bridging the models developed to describe glass sintering [9-10]. In glasses, the initial stage of sintering proceeds (up to a relative density $\rho_r \sim 0.8$) with a linear dependence on the ratio between surface tension and shear viscosity of the liquid phase, according to the Frenkel model [10]:

$$\frac{\Delta L}{L_0} = \frac{3\gamma}{8\eta(T)r} k_f t \quad (1)$$

where L_0 is the starting length of sample, ΔL the linear shrinkage after a sintering time t , $\eta(T)$ is the temperature dependent shear viscosity, γ is the glass-vapor surface tension, r is the starting particle radius and k_f is an adjustable factor.

As porcelain stoneware is sintered by partial vitrification – through the flow of an abundant liquid phase formed at high temperature – the relationship described by the Frenkel model can be applied to the densification of porcelain stoneware bodies too, as recently remarked by Conte and co-workers [11]. This study presents experimental data of porcelain stoneware sintering (obtained by hot stage microscopy), which reasonably match the densification rate calculated by Equation 1. Thus, the linear sintering rate is fundamentally governed by the surface tension/shear viscosity ratio of the liquid phase, and, consequently, the densification kinetics can be controlled through the chemical composition of the melt formed at high temperature.

It is possible to argue that the Frenkel model works for the prediction of the sintering behavior of typical porcelain stoneware batches. But what happens if the standard porcelain stoneware composition is changed by adding glassy wastes as raw materials? Is it still possible to reliably predict the sintering kinetics also in presence of high amounts of “fluxing” (Na, K, Ca, Mg) or “exotic” elements (e.g., Ba, Sr, Zn, B)? The present study will try to answer these questions by investigating the firing behavior of porcelain stoneware bodies containing glassy wastes. In particular, it will be evaluated if there is any deviation from the sintering model of porcelain stoneware, and the factors governing the effect of waste glasses on sintering mechanisms.

2. EXPERIMENTAL

The present study was conducted on six different porcelain stoneware batches: a benchmark mixture – consisting of 40wt% ball clays (plastic component), and 60wt% feldspathic fluxes and quartzous sands (non-plastic component) – and five glassy waste-based bodies with 20% wastes in replacement of non-plastic materials. Specifically, the wastes introduced in the batches derived from five different sources: bottle = B, PC-TV screen = S, lamp = L, glaze manufacturing = F, and porcelain stoneware grinding sludge = G.

The chemical composition of the raw materials used was determined by XRF (PW1400 Philips equipped with a W tube) and the batch chemistry was calculated considering the contribution by weight of each raw material (Table 1).

CHEMICAL COMPOSITION of the BODIES						
wt %	O	B	L	S	F	G
SiO ₂	70,81	70,61	70,73	68,74	68,22	70,66
TiO ₂	0,70	0,66	0,65	0,72	0,67	0,79
ZrO ₂	0,00	0,00	0,01	0,39	0,00	0,09
Al ₂ O ₃	19,93	17,17	16,88	17,09	18,76	20,24
Fe ₂ O ₃	0,74	0,72	0,68	0,66	0,68	0,89
MgO	0,44	0,78	0,96	0,43	0,60	0,46
CaO	0,86	2,58	1,59	0,82	2,65	0,92
ZnO	0,00	0,00	0,00	0,04	1,40	0,01
SrO	0,00	0,00	0,01	1,57	1,04	0,01
BaO	0,00	0,00	0,07	1,74	0,00	0,01
PbO	0,00	0,00	0,06	0,08	0,00	0,00
Na ₂ O	3,64	5,05	5,89	4,02	3,14	3,13
K ₂ O	2,87	2,43	2,48	3,69	2,84	2,78

Table 1.1. Chemical composition of the bodies

TECHNOLOGICAL PROPERTIES of UNFIRED TILES						
	O	B	L	S	F	G
Median particle size (μm)	5,1	6,1	5,6	5,3	6,3	4,5
Specific weight of raw body, SW ($\text{kg}\cdot\text{m}^{-3}$)	2633	2611	2604	2662	2641	2614
Bulk density of pressed body, BD ($\text{kg}\cdot\text{m}^{-3}$)	1858	1904	1848	1946	1908	1839
Dry open porosity (% by volume)	29,5	27,1	29,0	26,9	27,8	29,7
Springback ($\text{cm}\cdot\text{m}^{-1}$)	0,45	0,54	0,57	0,51	0,51	0,57
Relative density (1)	0,71	0,73	0,71	0,73	0,72	0,70
TECHNOLOGICAL PROPERTIES of FIRED TILES						
	O	B	L	S	F	G
Gresification temperature ($^{\circ}\text{C}$)	1240	1200	1160	1220	1200	1200
Firing shrinkage ($\text{cm}\cdot\text{m}^{-1}$)	5,0	3,9	5,1	1,8	5,5	6,5
Water absorption (% by weight)	0,73	0,14	0,13	0,14	0,18	0,50
Closed porosity (% by volume)	12,2	12,9	13,4	18,5	8,9	8,7
Bulk density ($\text{kg}\cdot\text{m}^{-3}$)	2211	2207	2189	2088	2364	2342
Specific weight of fired body, SW ($\text{kg}\cdot\text{m}^{-3}$)	2518	2535	2529	2562	2594	2555
Relative density (1)	0,88	0,87	0,87	0,81	0,91	0,92
PHASE COMPOSITION of FIRED BODIES						
	O	B	L	S	F	G
$^{\circ}\text{C}$	1240	1200	1160	1220	1200	1200
Quartz	21,7	14,0	15,9	13,3	16,0	23,0
Mullite	6,3	1,9	0,5	1,3	3,4	7,4
Plagioclase	0,8	10,4	11,3	3,0	9,3	2,2
K-feldspar	0,2	3,2	2,2	12,1	10,6	0,4
Amorphous	71,0	70,5	70,1	70,3	60,7	67

Table .21. Technological properties of the unfired and fired bodies and phase composition of the fired tiles.

Experiments were conducted on the six batches at laboratory scale, simulating the industrial tile-making process. The raw materials were mixed by wet milling in a porcelain jar using dense alumina media with a resulting mean particle diameter between 4.5 and 6.3 μm (Table 1). The slips were oven dried, de-agglomerated (hammer mill with grid of 500 μm) and manually granulated (sieve 2 mm, powder moisture $\sim 7\text{wt}\%$). Powders were pressed (40 MPa) into 110x55x5 mm tiles, dried in an electric oven at $105\pm 5^{\circ}\text{C}$ overnight and characterized for particle size distribution (ASTM C958), specific weight of powders (ASTM C604), bulk density (weight/volume ratio) and open porosity (Table 1).

Tiles were fired in an electric kiln at different maximum temperatures with a thermal cycle of about 60 min cold to cold. The firing temperature of each body corresponds to the gresification temperature, selected taking into account the temperature of maximum densification (T_{md} equivalent to the maximum shrinkage) and the temperature matching the standard requirement of water absorption $<0.5\%$ (TBIa) (Table 1).

The samples fired at the gresification temperatures followed the characterization described by Conte *et al.* [9; 11]. The phase composition was quantitatively assessed by X-ray powder diffraction (XRPD, D8 Advance; Bruker, Karlsruhe, Germany) in the $10\text{-}100^\circ 2\theta$ range, with a point detector equivalent time of 16 s per $0.02^\circ 2\theta$ scan step (LynxEye 1-dimensional detector; Bruker). A full profile modelling by Rietveld refinement was carried out with the GSAS-EXPGUI software package [12-13]. Following the Okada equation [14], the mullite stoichiometry was determined based on the length of the unit cell a -axis, which scales linearly with the amount of Al_2O_3 . The samples were admixed with corundum (20wt%) as internal standard to estimate the vitreous phase by difference, that is, 100% minus the sum of crystalline phases [15]. Based on the quantitative chemical and phase composition of fired body, the chemical composition of the vitreous phase was obtained by subtracting the contribution of each mineralogical phase, considering its stoichiometric formula, from the bulk chemistry (the resulting values were normalized to 100%). The physical properties at high temperature were estimated by predictive models based on the chemical composition of the liquid phase. The shear viscosity was calculated after Fluegel *et al.* [16], while surface tension was estimated by the Appen [17] and Dietzel [18] methods.

The sintering of the six batches was investigated by optical thermo-dilatometric analysis (TA ODP868, Faenza, Italy), which allows monitoring the thermal behavior by non-contact measurement of dimensional variations [19-20].

Data:

- P1. Start of viscous flow
- P2. Start of linear densification
- P3. End of linear densification
- P4. Maximum shrinkage
- P5. Shrinkage at the end of run

Process:

- P2-P1 = early densification
- P3-P2 = linear densification & sintering rate (Frenkel)
- P4-P3 = final densification & sintering rate (Mackenzie & Shuttleworth)
- P5-P4 = bloating index

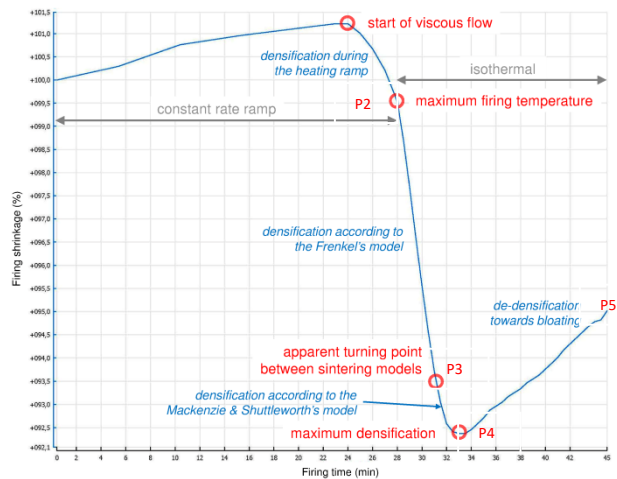


Figura 1. Ejemplo de ensayo isotérmico con adquisición de datos.

In this study, analyses were performed on specimens (6 x 6 x 6 mm in size) cut from the dry tiles. Tests were run under isothermal conditions at the different Tgr (reached with a gradient of 80°C/min), with dwell time of 30 minutes. The experimental results will be reported as in Figure 1, which shows the theoretical curve describing the different stage of the sintering. The initial sintering rates – describable by the Frenkel model – was calculated following the Equation 1. Input data were the starting mean particle size radius of bodies (Table 1) and the values of surface tension and shear viscosity at the various temperatures (Table 2). The equations were fitted to the given data by using the kf parameter as adjustable factors.

VITREOUS PHASE CHEMICAL COMPOSITION						
Wt %	O	B	L	S	F	G
SiO ₂	65,77	67,24	65,76	64,49	63,42	65,56
TiO ₂	0,99	0,93	0,93	1,03	1,10	1,18
ZrO ₂	0,00	0,00	0,01	0,56	0,00	0,14
Al ₂ O ₃	21,39	18,19	19,27	18,84	20,14	21,41
Fe ₂ O ₃	1,04	1,03	0,97	0,94	1,12	1,33
MgO	0,63	1,10	1,36	0,61	0,99	0,69
CaO	1,17	3,04	1,59	0,99	3,73	1,24
ZnO	0,00	0,00	0,00	0,06	2,31	0,02
SrO	0,00	0,00	0,01	2,24	1,72	0,02
BaO	0,00	0,00	0,11	2,47	0,00	0,01
PbO	0,00	0,00	0,09	0,12	0,01	0,00
Na ₂ O	5,03	5,79	6,90	5,32	3,75	4,37
K ₂ O	3,99	2,68	3,00	2,34	1,73	4,05
SHEAR VISCOSITY						
	O	B	L	S	F	G
	1240	1200	1160	1220	1200	1200
Log ₁₀ Pa·s	3,66	3,61	3,85	3,64	3,89	3,97
SURFACE TENSION						
	O	B	L	S	F	G
	1240	1200	1160	1220	1200	1200
mN m ⁻¹	337,2	343,7	347,2	342,4	357,7	343,4

Table 2. Vitreous phase chemical composition and physical properties.

Since the chemical composition of a porcelain stoneware tile can be described by the ternary diagram $\text{SiO}_2\text{-Al}_2\text{O}_3\text{-Na}_2\text{O}_{\text{eq}}$ (Fig. 2), it will be used to describe both the chemistry of the body and that of the vitreous phase.

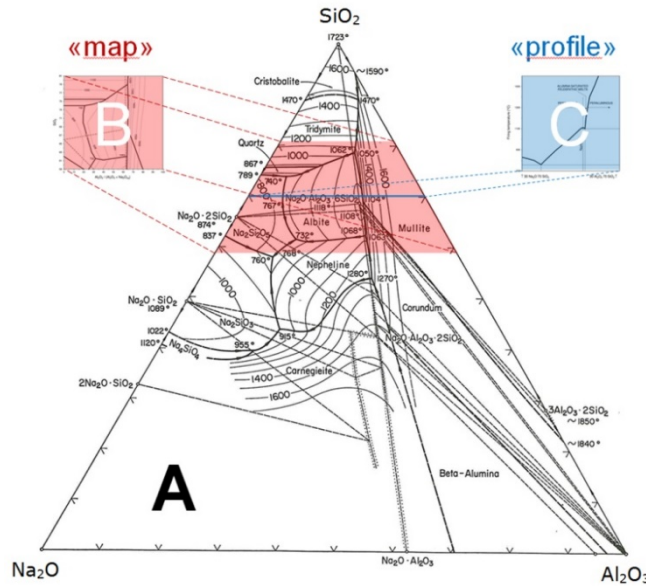


Figure 2. Ternary diagram $\text{SiO}_2\text{-Al}_2\text{O}_3\text{-Na}_2\text{O}_{\text{eq}}$ (A). The part highlighted in red (B) is enlarged in figure 3a, while the blue line (C) is the intersection with the profile of figure 3b.

$\text{Na}_2\text{O}_{\text{eq}}$ accounts for the contribution of other elements acting as glass network modifiers or as charge compensators of Al^{3+} ions in tetrahedral coordination in the glassy phase. Specifically, $\text{Na}_2\text{O}_{\text{eq}}$ was calculated as the sum $\text{Na}_2\text{O} + \text{MgO} + \text{CaO} + \text{K}_2\text{O} + \text{ZnO} + \text{SrO} + \text{BaO} + \text{PbO}$, taking care to express the data as Na_2O equivalent using the following molar ratios: 1.538 (MgO), 1.105 (CaO), 0.658 (K_2O), 0.762 (ZnO), 0.598 (SrO), 0.404 (BaO), 0.278 (PbO).

3. RESULTS AND DISCUSSION

The introduction of different raw materials, such as glassy wastes, in a typical porcelain stoneware body caused a change in the bulk chemical composition (Table 1), which determined a different equilibrium among the phases.

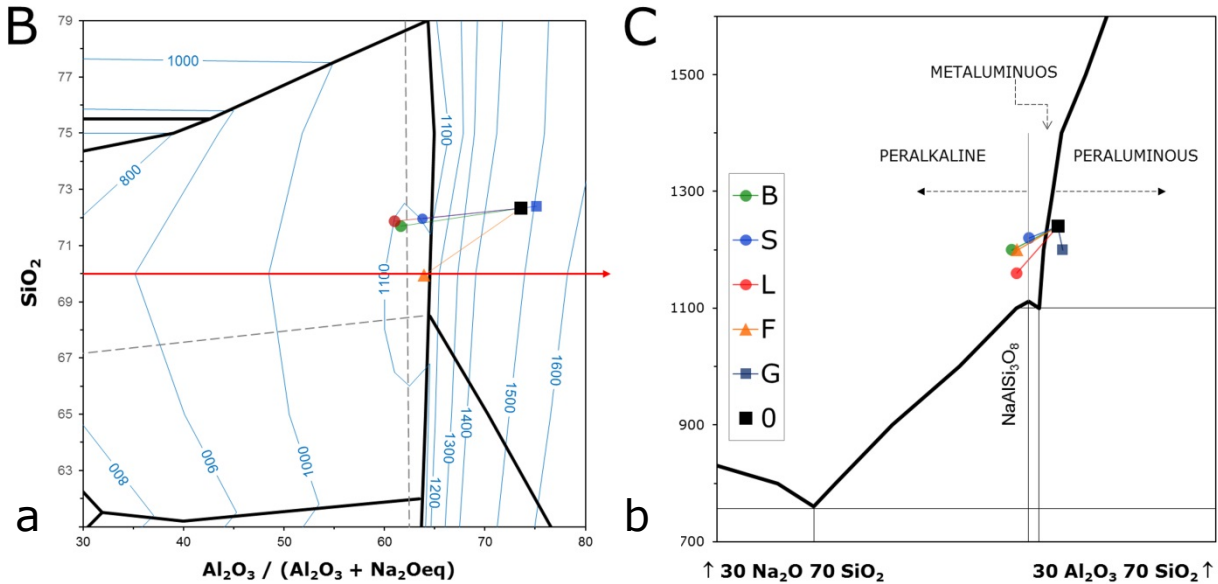


Figure 3. Chemical composition of the porcelain stoneware bodies (a = B of fig. 2) and chemical composition of the vitreous phases (b = C of fig. 2).

This can be easily described by plotting the chemistry of the bodies in the SiO₂-Al₂O₃-Na₂O phase diagram of figure 3a. It is possible to observe that the benchmark 0 and the sample G (made up of 20% porcelain stoneware grinding sludge) lie in the mullite stability field. This is mirrored by the phase composition of the fired samples showing higher mullite content (6.3-7.4wt%, respectively) with respect to the other batches containing glassy wastes (0.5-3.4wt% mullite). On the other hand, samples S, F, L and B, lying in the albite (feldspars) stability field, show higher levels of feldspars in the fired bodies (13.5-19.9wt%), compared to the 0 and G batches (1-2.6wt%, respectively). More in detail, batches F and S, standing really near to the cotectic, are the most enriched in final feldspars content.

The change in the bulk chemistry and phase composition of the bodies is also mirrored in the chemical composition of the vitreous phases formed during the heating treatment of the batches. The chemistry of the liquid phase determines its degree of polymerization, and, consequently, its physical properties, in particular viscosity. Besides the well-known role of certain elements in the melt structure, like Si as glass network former (GNF) or alkalis and alkali earths as glass network modifiers (GNM) or charge compensators (CCA), the role of specific elements, called glass network intermediates (GNI), can be crucial. Among them, the most relevant is Al³⁺, which can be incorporated either as GNF or GNM. As GNF it has a four-fold oxygen coordination, up to the stoichiometric ratio between alumina and alkaline or alkaline-earth oxides in feldspars, which act as charge compensators (CCA). Otherwise, Al³⁺ acts as GNM when the composition becomes peraluminous and coordination with oxygen turns 5 or higher

or gives rise to triclusters. The vitreous phase chemical compositions of our samples are very close to feldspar stoichiometry, represented in figure 3b by the meta-aluminous line. This means that the Al^{3+} present in the melt is mainly four-fold oxygen coordinated, acting as GNF. On the other hand, a further introduction of glassy wastes will turn the melt peralkaline, causing a higher degree of depolymerization (as observed for samples with 40-60wt% of glassy wastes – authors' unpublished data) and a loss of viscosity at the same temperature.

The sintering behavior of the bodies under investigation is summarized in Figure 4, where the shrinkage curves versus time are plotted for firings at temperatures between 1160 and 1240°C (for the gresification temperature of each sample see Table 1).

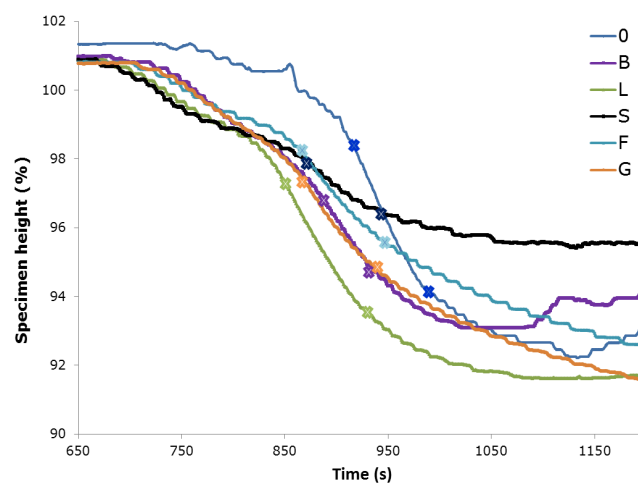


Figure 4. Shrinkage as a function of time.

The introduction of wastes implies a different sintering behavior with respect to the benchmark. The temperatures at which the viscous flow starts in glassy waste-based bodies are lower, but the linear stages of the sintering, where a constant rate densification took place, are shorter. In other words, the portion of the process that can be predicted by the Frenkel model is reduced from 50% of the benchmark, down to 25% of the S and G batches. This is because in the glassy waste-based bodies a substantial part of the densification (up to 56% of the process) takes place during the heating ramp, before reaching the isotherm. It is also possible to observe that samples S and B show a peculiar behavior, with the lowest shrinkage of the whole set, as also shown by the lower degree of densification (difference between relative density of the fired tiles and unfired ones, Table 1).

Figure 5 reports the sintering rate of the linear stage of the process, corresponding to the isotherm. The sintering rate describes the viscous flow sintering kinetics, so the higher the rate, the faster the densification.

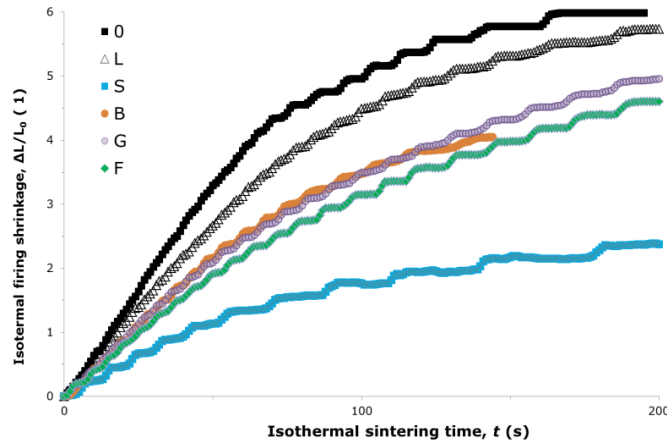


Figure 5. Linear shrinkage in isothermal condition as a function of time.

It seems that the introduction of glassy wastes does not accelerate the densification, since the benchmark exhibits the highest rate of the set. Anyway, it is important to remember that in these batches containing wastes an early densification occurs during the heating ramp, in non-isothermal condition. This means that the sintering kinetics of the benchmark is faster just in the linear stage of the process, while the other batches start before their densification and in this stage their kinetics are slower.

In order to check the reliability of the Frenkel model to predict the sintering kinetics of porcelain stoneware batches, the experimental linear rates obtained by the optical thermo-dilatometer were compared with the sintering rates calculated by the Frenkel model as reported in Figure 6.

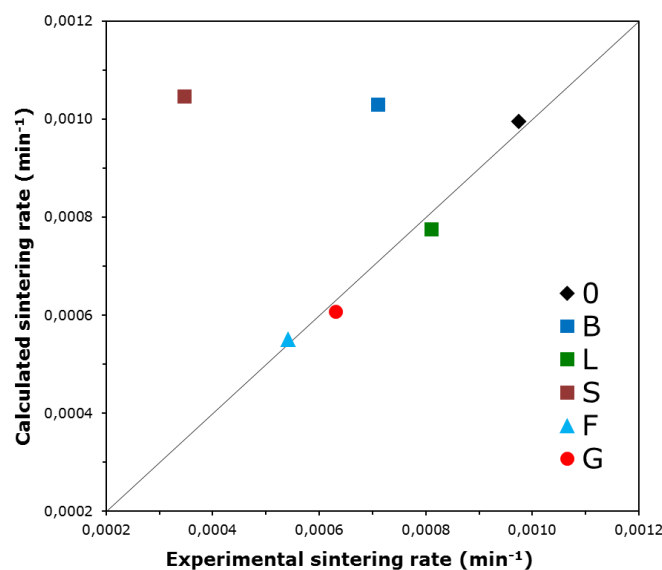


Figure 6. Calculated versus experimental sintering rates (linear stage) of the different batches.

Four of the six samples show a reasonable match between the experimental and calculated data. However, batches B and S are characterized by lower experimental sintering rates with respect to the calculated values. This means that the relationship between surface tension and shear viscosity of the liquid phase fails to predict accurately the sintering rate, perhaps due to lack in the estimation of other factors, such as closed porosity. In the case of batch S, in fact, the densification of the sample is interrupted by the development of a large quantity of closed pores (see Table 1), which arrests the sintering.

4. CONCLUSIONS

The substitution of feldspathic fluxes with waste glasses determines a clear change in the firing behavior that goes beyond densification kinetics, involving phase composition and chemical features of the vitreous phase. Waste glasses lower the temperature at which the densification starts, and extend the early stage occurring before a constant rate sintering takes place. In some cases, the deviation is important and entails a lower sintering efficiency: the maximum density achieved with bottle or screen glasses, in particular, is much lower than the benchmark. Once the different phase compositions are considered, as well as the composition and physical properties of the vitreous phase, it is possible to predict the sintering rate by the Frenkel model. However, this prediction has less significance in bodies containing waste glass, because the constant rate stage represents just 25% of total shrinkage, at variance with the waste-free body (50%). In two cases (B and S) the model fails, predicting a much higher sintering rate than the observed one. The reasons for these different firing behaviors have to be sought in the structural changes in the melt. In the waste-bearing bodies, the addition of alkalis and alkaline earths – not counterbalanced by alumina, as occurs when feldspars are used – determines a shift from a slightly peraluminous melt (waste-free batch) towards metaluminous and slightly peralkaline melts. This shift probably reflects important aspects, such as the densification degree, along with sintering kinetics.

5. ACKNOWLEDGEMENTS

This work has been performed in the frame of "Sustainable materials for the recovery and realization of new buildings" MATER_SOS project, funded by Emilia Romagna region (Italy) with European funds (POR-FESR Asse 1 Ricerca e Innovazione, Azione 1.2.2, www.matersos.it (CUP E32I16000020007)).

6. REFERENCES

- [1] Baraldi L., "World production and consumption of ceramic tiles". *Ceramic World Review*, 128 (2018) 58-72.
- [2] Ferrari A., Volpi L., Pini M., Siligardi C., García-Muina F., Settembre-Blundo D., "Building a sustainability benchmarking framework of ceramic tiles based on Life Cycle Sustainability Assessment (LCSA)". *Resources*, 8 (2019) 11.
- [3] "Industrie produttrici di piastrelle di ceramica. Fattori di impatto e prestazioni ambientali". *Confindustria Ceramica, Rapporto 2010-2013*.
- [4] Andreola F., Barbieri L., Lancellotti I., Leonelli C., Manfredini T., "Recycling of industrial wastes in ceramic manufacturing: State of art and glass case studies". *Ceramics International*, 42 (2016) 13333-13338.
- [5] Matteucci F., Dondi M., Guarini G., "Effect of soda-lime glass on sintering and technological properties of porcelain stoneware tiles". *Ceramics International*, 28 (2002) 873-880.
- [6] Tucci A., Esposito L., Rastelli E., Palmonari C., Rambaldi E., "Use of soda-lime scrap-glass as a fluxing agent in a porcelain stoneware tile mix". *Journal of the European Society*, 24 (2004) 83-92.
- [7] Rambaldi E., Carty W.M., Tucci A., Esposito L., "Using waste glass as a partial flux substitution and pyroplastic deformation of a porcelain stoneware tile body". *Ceramics International*, 33 (2007) 727-733.
- [8] Raimondo M., Zanelli C., Matteucci F., Guarini G., Dondi M., Labrincha J.A., "Effect of waste glass (TV/PC cathodic tube and screen) on technological properties and sintering behavior of porcelain stoneware tiles". *Ceramics International*, 33 (2007) 615-623.
- [9] Conte S., Zanelli C., Ardit M., Cruciani G., Dondi M., "Predicting viscosity and surface tension at high temperature of porcelain stoneware bodies: a methodological approach". *Materials*, 11 (2018) 2475
- [10] Müller R., Reinsch S. (2012). Viscous phase silicate processing. In: Bansal N.P. & Boccaccini A.R. (eds.), *Processing Approaches for Ceramics and Composites*, Wiley, 75-144.
- [11] Conte S., Zanelli C., Ardit M., Cruciani G., Dondi M., "Phase evolution during reactive sintering by viscous flow: disclosing the inner workings in porcelain stoneware firing", in preparation.
- [12] Larson A. C., Von Dreele R. B., "GSAS, General Structure Analysis System". Los Alamos National Laboratory, Los Alamos, NM, (1988) 86-748.
- [13] Toby B. H., "EXPGUI, a graphical user interface for GSAS". *Journal of applied crystallography*, 34 (2001) 210-213.
- [14] Ban T., Okada K., "Structure refinement of mullite by the Rietveld method and a new method for estimation of chemical composition". *Journal of the American Ceramic Society*, 75(1), (1992) 227-230.
- [15] Gualtieri A. F., Riva V., Bresciani A., Maretti S., Tamburini M., Viani A., "Accuracy in quantitative phase analysis of mixtures with large amorphous contents. The case of stoneware ceramics and bricks". *Journal of Applied Crystallography*, 47(3), (2014) 835-846.
- [16] Fluegel A., "Glass viscosity calculation based on a global statistical modelling approach". *Glass Technol. PartA* 48 (2007) 13-30.
- [17] Appen A.A., "Chemistry of Glass (Russ.)". *Khimiya: Leningrad, Russia*, 351 (1974)
- [18] Dietzel A., "Relation between the surface tension and the structure of molten glass". *Kolloid-Z.*, 100 (1942) 368-380.
- [19] Lara C., Pascual M. J., Prado M. O., Durán A., "Sintering of glasses in the system RO-Al₂O₃-BaO-SiO₂ (R= Ca, Mg, Zn) studied by hot-stage microscopy". *Solid State Ionics*, 170 (2004) 201-208.
- [20] Karamanov A., Dzhantov B., Paganelli M., Sighinolfi D., "Glass transition temperature and activation energy of sintering by optical dilatometry". *Thermochimica acta*, 553 (2013) 1-7.